Title: A conserved membrane protein negatively regulates Mce1 complexes in mycobacteria

Authors: Yushu Chen[a], Shu-Sin Chng[a,b,*]

Affiliations:

[a] Department of Chemistry, National University of Singapore, Singapore 117543.

[b] Singapore Center for Environmental Life Sciences Engineering, National University of Singapore (SCELSE-NUS), Singapore 117456.

* To whom correspondence should be addressed. Email: chmchngs@nus.edu.sg

Author contributions: Y.C. and S.-S.C. designed research; Y.C. performed research; Y.C. and S.-S.C. analyzed data; Y.C. and S.-S.C. wrote the paper.

Competing Interest Statement: The authors declare that no competing interests exist.

Classification: Biological Sciences (Biochemistry)

Keywords: mammalian cell entry, ABC transporter, fatty acid uptake, negative regulator

This PDF file includes

Main Text

Figures 1 to 5

Abstract

Tuberculosis (TB) remains one of the deadliest infectious diseases, posing a serious threat to global health. *Mycobacterium tuberculosis*, the causative agent of TB, is an intracellular pathogen that relies on various mechanisms to survive and persist within the host environment. Among the many virulence factors that contribute to pathogenesis, mycobacteria encode Mce systems, putative transporters that are important for lipid uptake. The molecular basis for Mce function(s) is poorly understood. To gain insights into the composition and architecture of mycobacterial Mce systems, we characterized the putative Mce1 complex involved in fatty acid transport. Using affinity purification, we show that the Mce1 system in *Mycobacterium smegmatis* is an ATP-binding cassette transporter complex comprising YrbE1A/B as heterodimeric transmembrane domains (TMDs) and MceG as nucleotide-binding domains (NBDs), associated with possible heterohexameric assemblies of MCE-domain substrate-binding proteins. We demonstrate that Msmeg_6540 and Mce1A are functionally redundant homologs, likely forming distinct Mce1 complexes that contribute to fatty acid uptake. Finally, we establish that the membrane protein Msmeg_0959, herein renamed to Mce1N, negatively regulates Mce1 function by blocking MceG access to YrbE1B. This regulatory mechanism is conserved in *M. tuberculosis* Mce1N (Rv0513). Our work offers molecular understanding of Mce complexes, shedding light on lipid metabolism and its regulation in mycobacteria.

42 **Introduction**

43 Tuberculosis (TB) has been one of the top killers among single infectious diseases in humans, alone
44 claiming 1.3 million lives out of 10 million new cases in 2020 (1). Apart from the active cases, it is estimated
45 that one quarter of the world population are carriers of latent TB, which may progress into active infections
46 (2). TB is primarily caused by *Mycobacterium tuberculosis*, an organism known for its ability to adapt to
47 the host environment and modulate the host immune system (3). Its success as a pathogen can be owed
48 to diverse virulence factors encoded in the genome of *M. tuberculosis*. In particular, many of these
49 virulence factors promote host adaptation by contributing to the acquisition and catabolism of important
50 nutrients including metals, sugars and lipids (4).

51 Mycobacterial *mce* operons have been recognized as a group of virulence factors important for lipid
52 uptake (5). These operons are widespread throughout the *Mycobacterium* genus, with different numbers
53 present in different species (6). *Mycobacterium smegmatis,* an environmental microorganism, contains six
54 *mce* operons*,* while *Mycobacterium leprae*, the causative agent of leprosy, has only one such operon
55 (*mce1*) in its highly degenerate genome. *M. tuberculosis* contains four *mce* operons, individually important
56 determinants of virulence and collectively critical for pathogenesis (7-10). For example, the *mce1* and
57 *mce4* operons are implicated in fatty acid and cholesterol uptake, respectively (9, 11, 12). In general, an
58 *mce* operon consists of eight genes, two *yrbE* (e.g., *yrbE1A/B*) and six *mce* genes (e.g., *mce1A–F),* with
59 different numbers of accessory genes (6) that may be required for function (12, 13) (e.g., *mam1A–D* after
60 the *mce1* operon). Furthermore, a gene encoding a transcriptional regulator (e.g., *mce1R*) can be found
61 upstream of some *mce* operons (6, 14, 15) (*SI Appendix*, Fig. S1). Our understanding of how these
62 operons facilitate lipid uptake is limited.

63 It is believed that *mce* operons encode ATP-binding cassette (ABC) transporters that are analogous
64 to the MlaFEDB complex in Gram-negative bacteria (6, 16), which is important for retrograde transport of
65 phospholipids (17, 18). In MlaFEDB, MlaF, MlaE and MlaD represent the nucleotide-binding domains
66 (NBDs), transmembrane domains (TMDs), and substrate-binding proteins (SBPs), respectively (19, 20).
67 In Mce systems, YrbEA/Bs and MceA–Fs would form the corresponding TMDs and SBPs based on
68 homology; here, MceG, a protein not encoded within *mce* operons, is thought to constitute the NBDs that
69 energize all these putative transporters (21, 22). MlaD and MceA–F all contain a single mammalian cell

70 entry (MCE) domain. Interestingly, MlaD and other MCE-domain proteins, such as PqiB and YebT/LetB,
71 have been shown to form homohexamers that provide a hydrophobic tunnel each, presumably for lipid
72 substrate transport (19, 20, 23, 24). The fact that *mce* operons encode six Mce proteins MceA–F hints at
73 the possible formation of heterohexameric MCE assemblies within each putative transporter. Despite
74 similarities to MlaFEDB, however, there has been a lack of biochemical studies on mycobacterial Mce
75 systems, and their exact compositions and overall architectures remain unknown.

76 Here, we biochemically characterized the putative Mce1 complex in *M. smegmatis.* We demonstrate
77 that Mce1 is an ABC transporter comprising a core complex of YrbE1A/B-MceG, associated with a likely
78 heterohexamer of Mce1A–F. We reveal that Msmeg_6540 is a functional homolog that can possibly
79 replace Mce1A in the complex, and both proteins contribute to the fatty acid uptake function of Mce1.
80 Furthermore, we identify Msmeg_0959, herein renamed to Mce1N, as a negative regulator of the Mce1
81 system; it prevents MceG from associating with the complex via competitive binding to YrbE1B, thereby
82 modulating transport activity. Our work provides critical insights into the architecture, function and
83 regulation of Mce systems in mycobacteria.

84

85 **Results**

86 **Key proteins encoded in the *mce1* operon co-purify as a complex**

87 To probe the composition of the putative Mce1 complex, we expressed His-tagged YrbE1A or YrbE1B
88 in *M. smegmatis* using an integrative plasmid and conducted affinity purification following cell lysis and
89 detergent extraction from total membranes. This was done in a strain that presumably up-regulates the
90 *mce1* operon due to the lack of Mce1R, a known negative regulator (14). We found that His-tagged YrbE1B,
91 but not YrbE1A, pulled down two distinct protein bands at ~45 and ~19 kDa (Fig. 1). Tandem mass
92 spectrometry (MS/MS) sequencing of the excised bands indicated that they were MceG (39.0 kDa) and a
93 protein of unknown function, Msmeg_0959 (19.1 kDa), respectively. We did not observe additional bands
94 corresponding to other expected members of the Mce1 complex, possibly due to low cellular levels, or
95 instability of the complex *ex vivo*. To detect potential low abundance proteins specifically co-purified with
96 His-tagged YrbE1B, we directly subjected entire gel lanes divided into two sections to MS/MS protein
97 identification. Remarkably, this facilitated the detection of all other putative Mce1 components, including

98 YrbE1A and Mce1A–F, similar to a recent report identifying YrbE4A/B, Mce4A–F and MceG as components
99 of the Mce4 complex (13). Interestingly, a seventh MCE-domain protein Msmeg_6540 (6) was also co-
100 purified with His_6-YrbE1B, while none of the putative Mce-associated membrane proteins (Mam1A–D) was
101 identified. Our data suggest that the Mce1 complex likely comprises the core ABC transporter YrbE1A/B-
102 MceG associated with a presumed heterohexamer of MCE-domain proteins.
103

104 **Msmeg_6540 and Mce1A are two redundant components of the Mce1 system**

105 Msmeg_6540 shares 80% primary sequence identity with Mce1A, compared to less than 20% with
106 other MCE-domain proteins in the Mce1 complex and ~25% with MceA proteins in other putative *M.*
107 *smegmatis* Mce complexes (*SI Appendix*, Table S4). Another Mce1A paralog Msmeg_5818 (6), which is
108 only 60% identical, was not co-purified with His-tagged YrbE1B (Fig. 1). This suggests that Msmeg_6540
109 could be a functional homolog of Mce1A. To study the role of Msmeg_6540, we tested the effects of
110 deleting *msmeg_6540* on fatty acid uptake, a key function of the Mce1 complex (11, 12). Deletion of
111 *yrbE1A/B* or *mceG* resulted in reduced [^{14}C]-palmitic acid uptake (Fig. 2A), and retarded cell growth
112 specifically when palmitate was the sole carbon source (Fig. 2B). Interestingly, we found that [^{14}C]-palmitic
113 acid uptake was less efficient in cells lacking either *mce1A* or *msmeg_6540*, and in fact further reduced in
114 the Δ*mce1A*Δ*6540* double mutant, comparable to levels in Δ*yrbE1A/B* or Δ*mceG* cells (Fig. 2A). In addition,
115 while both single deletion mutants exhibited slower growth when using palmitate as the sole carbon source,
116 the Δ*mce1A*Δ*6540* strain grew at an even lower rate, again similar to Δ*yrbE1A/B* or Δ*mceG* strains (Fig.
117 2B). Our results therefore reveal that Mce1A and Msmeg_6540 are functionally redundant. Curiously,
118 removing Msmeg_6540 has a stronger impact on fatty acid uptake than removing Mce1A, suggesting
119 Mce1 complexes containing Msmeg_6540 in place of Mce1A could play a more important role in *M.*
120 *smegmatis*.
121

122 **YrbE1A/B-MceG constitute the core ABC transporter**

123 Despite extensive efforts, we were not successful in over-expressing the *mce1* operon along with
124 *mceG* in *E. coli* and purifying the full Mce1 complex. Instead, we were able to isolate the core ABC
125 transporter when we co-expressed YrbE1A, His-tagged YrbE1B and MceG. This complex eluted as a

126 single peak on size exclusion chromatography (Fig. 3A); we showed that the purified complex exhibits ATP
127 hydrolytic activity (Fig. 3B), implying proper assembly of YrbE1A/B-MceG. Interestingly, we found that His-
128 tagged YrbE1B alone, but not YrbE1A, could pull down MceG when co-expressed in *E. coli*, indicating that
129 the TMD-NBD interactions are mainly mediated through YrbE1B (Fig. 3C). Consistent with this idea, an
130 AlphaFold2 structural model of the YrbE1A/B-MceG complex (25-27), which resembles the homologous
131 MlaFE structure from Gram-negative bacteria (RMSD=2.934 Å; *SI Appendix*, Fig. S2) (28), presented a
132 smaller buried area between MceG and YrbE1A (699 $Å^2$) compared to YrbE1B (837 $Å^2$) (Fig. 3D and *SI*
133 *Appendix*, Table S5). We conclude that the TMDs and NBD proteins of the Mce1 system interact
134 asymmetrically to form a stable functional ABC transporter.
135
136 **Msmeg_0959 is a negative regulator of Mce1**
137 In addition to MceG, Msmeg_0959 was another protein abundantly co-purified with His-tagged
138 YrbE1B expressed in *M. smegmatis*. Msmeg_0959 is a putative conserved membrane protein with
139 unknown function; it contains two predicted transmembrane helices (TM1: W39-G59; TM2: L65-T90) and
140 a C-terminal cytoplasmic domain (S91-P178) (*SI Appendix*, Fig. S3). We initially hypothesized that it might
141 function to stabilize the Mce1 complex, analogous to the role of the cytoplasmic protein MlaB in the Gram-
142 negative MlaFEDB complex (19). To test this idea, we attempted to isolate a stable complex containing
143 YrbE1A/B, MceG and Msmeg_0959. To our surprise, when these four proteins were co-expressed and
144 purified from *E. coli*, Msmeg_0959, but noticeably not MceG, was co-purified with His-tagged YrbE1B (Fig.
145 4A). This observation suggests that Msmeg_0959 may destabilize the Mce1 complex instead. In support
146 of this notion, when Msmeg_0959 was overexpressed in *M. smegmatis*, much less MceG was co-purified
147 with His-tagged YrbE1B (Fig. 4B). We conclude that Msmeg_0959 may disrupt YrbE1A/B-MceG
148 interactions.
149 Since TMD-NBD interaction within the Mce1 complex is largely mediated through YrbE1B, we
150 presumed that Msmeg_0959 directly interacts with YrbE1B. We generated an AlphaFold2 structural model
151 comprising YrbE1B and Msmeg_0959 (25-27), predicting possible interactions between the
152 transmembrane domain of Msmeg_0959 and that of YrbE1B opposite its dimerization surface with YrbE1A
153 (Fig. 4C). The structural model revealed that the cytoplasmic domain of Msmeg_0959 may contact a short

154 helix of YrbE1B sitting at the membrane-water boundary. This helix may be a determinant of the interaction
155 between YrbE1B and Msmeg_0959 since the amino acid sequence of this region is very different from that
156 in YrbE1A, which did not pull down Msmeg_0959 in *M. smegmatis* (*SI Appendix*, Fig. S4). Mutating part
157 of this helix (RLVAEIGMGT) to a flexible loop (GGSSG) did not affect the stability of the YrbE1A/B-MceG
158 complex *in vitro*. However, this mutation prevented co-purification of Msmeg_0959 with His-tagged YrbE1B
159 from *E. coli*, at the same time alleviating the destabilizing effect of Msmeg_0959 on YrbE1A/B-MceG
160 interactions (Fig. 4A). Notably, overlay of the models of YrbE1B-Msmeg_0959 and YrbE1A/B-MceG
161 highlighted substantial steric clashes between MceG and the cytoplasmic domain of Msmeg_0959 (Fig.
162 4C), indicating that their respective interactions with YrbE1B are likely competitive and mutually exclusive.
163 Taken together, our results establish that Msmeg_0959 specifically binds YrbE1B and prevents association
164 of the NBD (MceG) to this ABC transporter.

165 Our biochemical experiments suggest that Msmeg_0959 may be a negative regulator of the Mce1
166 complex. Consistent with this idea, Msmeg_0959 overexpression inhibited [^{14}C]-palmitic acid uptake in WT
167 cells, but not residual uptake observed in Δ*yrbE1A/B* cells (Fig. 4D). Furthermore, we found that
168 overexpression of Rv0513, the *M. tuberculosis* homolog of Msmeg_0959, in *M. smegmatis* similarly
169 reduced the amount of MceG associated with YrbE1B (Fig. 4B), and slowed down [^{14}C]-palmitic acid
170 uptake (Fig. 4D). In contrast, overexpression of Ml2418c, the truncated *M. leprae* homolog lacking a large
171 portion of the C-terminal cytoplasmic domain (*SI Appendix*, Fig. S3), had no such effects (Fig. 4B and D).
172 We therefore conclude that Msmeg_0959/Rv0513, herein renamed to Mce1N (Mce1 negative regulator),
173 inhibits the fatty acid uptake function of the Mce1 transporter(s) via a conserved mechanism that involves
174 prevention of YrbE1B-MceG interaction.

175

176 **Discussion**

177 In this study, we set out to characterize the Mce1 complex in *M. smegmatis*. We have shown that the
178 complex likely comprises the core inner membrane ABC transporter YrbE1A/B-MceG, associated with a
179 putative heterohexamer composed of Mce1A–F. Interestingly, we have found that Msmeg_6540, a
180 homolog of Mce1A, can also be co-purified as part of the Mce1 complex, and have demonstrated that it is
181 functionally redundant with Mce1A in fatty acid uptake. Furthermore, we have discovered a negative

182 regulator of the Mce1 complex, Mce1N, which physically hinders the dominant TMD-NBD interaction (i.e.,
183 YrbE1B-MceG) in the ABC transporter. Our work provides novel insights into the architecture and
184 regulation of mycobacterial Mce complexes.

185 Based on analogy to other MCE-domain proteins, such as MlaD, PqiB (20) and YebT/LetB (23, 24)
186 involved in lipid transport in Gram-negative bacteria (*SI Appendix*, Fig. S5*A*), Mce1A–F likely form a
187 hexamer. Each of these Mce proteins contains a single MCE domain (like MlaD) and an extended helical
188 domain (like PqiB), followed by the presence of an additional C-terminal domain of varied sizes. According
189 to AlphaFold2 prediction (25, 26, 29), Mce1A–F can indeed form a heterohexamer (*SI Appendix*, Fig. S5*B*).
190 In contrast, a homohexameric model of Mce1A alone could not be generated. In the AlphaFold2 model,
191 the heterohexamer adopts an architecture that comprises a hexameric MCE ring connected to a tube
192 formed by a bundle of the helical domains; a continuous hydrophobic tunnel runs through the entire
193 assembly that might extend across the periplasm (Fig. 5 and *SI Appendix*, Fig. S5*B* and *C*), consistent
194 with its function in fatty acid uptake. In this predicted model, the C-terminal domains of the six Mce proteins
195 organize to form a possible substrate entry point at the tip (*SI Appendix*, Fig. S5*B*). Interestingly, *M.*
196 *smegmatis* possesses Msmeg_6540 as a functional homolog of Mce1A, hinting towards the presence of
197 two variants of Mce1 complexes (6), containing Mce1B–F and either Mce1A or Msmeg_6540 (Fig. 5).
198 Differences between the primary sequences of Mce1A and Msmeg_6540 lie mainly in the extreme C-
199 terminal domain, with differing residues mapped to both the exterior and interior of the 'substrate entry
200 point' in the AlphaFold2 models (*SI Appendix*, Fig. S5*D*). We propose that Mce1 complexes containing
201 either Mce1A or Msmeg_6540 may have distinct substrate specificities, perhaps advantageous for an
202 environmental microorganism like *M. smegmatis*.

203 Despite the fact that there are known ABC transporters with heterodimeric TMDs, it has not been
204 appreciated that such asymmetry can give rise to major differences in affinity between each TMD and NBD
205 pair—in the case of the Mce1 transporter, the NBD dimer may be predominantly recruited by YrbE1B. This
206 might be applicable to other ABC transporters with heterodimeric TMDs since TMD-NBD interfaces of
207 different areas were also observed within some of them (*SI Appendix*, Table S5). That TMD-NBD
208 association in the Mce1 transporter relies on the YrbE1B-MceG interaction offers a compelling reason why
209 the negative regulator Mce1N also selectively binds YrbE1B. Based on our modeling and biochemical data,

210 the cytoplasmic domain of Mce1N likely interacts with YrbE1B extensively at a short helix between the
211 latter's N-terminal amphipathic interface helix and TM1. This short helix is nominally a part of TM1 but is
212 presented at an angle due to a kink introduced by a flexible loop within TM1. Remarkably, this structural
213 feature may be exclusively conserved across YrbEBs, but not YrbEAs (*SI Appendix*, Fig. S6). This raises
214 an interesting possibility that beyond the most conserved Mce1 complex, Mce1N may also regulate
215 additional Mce systems by binding to the corresponding YrbEB, perhaps providing a way to redistribute
216 MceG among all Mce systems.

217 The discovery of a negative regulator that competes with the NBD for binding to the TMDs may be
218 unique to Mce complexes, as known regulatory mechanisms for ABC transporters typically involve
219 modulation of ATPase activity instead of removing the NBD from the complex (19, 30-34). How and when
220 the Mce1 complex is modulated would directly depend on the levels of Mce1N (Fig. 5), which is highly
221 conserved across the *Mycobacterium* genus (present in both fast- and slow-growing, pathogenic and non-
222 pathogenic species). We note that *mce1N* may be in an operon together with four upstream essential
223 genes involved in porphyrin biosynthesis (*hemACDB*). Porphyrin biosynthesis has been reported to
224 increase, suggesting possible up-regulation of Mce1N (Msmeg_0959), when *M. smegmatis* cells enter
225 dormancy (35). In this situation, negative regulation by Mce1N might be a strategy that cells use to inhibit
226 some Mce complexes to conserve ATP. Alternatively, Mce1N levels may correlate with the need for lipid
227 uptake. Outside the host, where fatty acid substrates may be scarce, it might be preferable for
228 mycobacterial cells to keep the Mce1 system in a routinely OFF state and avoid futile ATP hydrolysis.
229 During infection, however, cells may require a fully active Mce1 complex to utilize host fatty acids. We do
230 not yet know of any environment-dependent regulation of Mce1N. However, it is noteworthy that in *M.*
231 *leprae,* which possesses Mce1 as the only Mce system (6), Mce1N (Ml2418c) lacks the C-terminal
232 cytoplasmic domain and is likely non-functional. Consistently, we have shown that Ml2418c was unable to
233 inhibit the Mce1 complex when overexpressed in *M. smegmatis* (Fig. 4). Combined with the fact that
234 *mce1R,* the gene encoding the transcriptional repressor of the *mce1* operon (*SI Appendix*, Fig. S1), is
235 absent in *M. leprae*, the pathogen may have lost its ability to down-regulate the Mce1 system, which can
236 facilitate constitutive fatty acid uptake during its obligate parasitic life cycle.

237 We have uncovered a new regulatory mechanism for Mce1 (Fig. 5), and potentially other Mce systems,

238 which may have implications for how mycobacterial cells coordinate lipid uptake processes. Despite the
239 presence of a transcriptional regulator for some *mce* operons (*SI Appendix*, Fig. S1), all Mce transporters
240 apparently share the same ATPase MceG (22). This indicates that mycobacterial cells have the ability to
241 modulate the levels of each complex, yet adjust their activities simultaneously. In the same vein, we
242 speculate that Mce1N could also be a shared negative regulator to counter MceG binding/activation, and
243 primarily functions to deactivate all Mce complexes simultaneously. Whether Mce1N has preferences for
244 specific Mce systems remains to be examined. Nevertheless, it likely contributes significantly to the overall
245 regulation towards maintaining a balanced metabolic flux of different lipid substrates required for
246 mycobacterial survival (12, 36), which may involve other yet-to-be-identified uptake transporters beyond
247 Mce systems (37).
248

249 **Materials and Methods**

250 **Affinity purification**

251 Harvested *M. smegmatis* or *E. coli* cells were resuspended in cold TBS (Tris-buffered saline, 20 mM Tris-
252 HCl pH 8.0, 150 mM NaCl) containing lysozyme, phenylmethylsulfonyl fluoride, and DNase I, and lysed
253 using a French Press (GlenMills) at 20,000 psi. After removal of unbroken cells by centrifugation, the
254 supernatant was subjected to ultra-centrifugation at 95,000 x *g* for 45 min. Membrane proteins were
255 extracted from the pellet using TBS-A (TBS containing 5 mM $MgCl_2$ and 10% glycerol) with 1% n-dodecyl-
256 β-D-maltoside (DDM). The suspension was subjected to a second round of ultra-centrifugation at 89,000
257 x *g* for 45 min. The supernatant was loaded onto TALON metal affinity resin (Takara Bio) pre-equilibrated
258 with TBS. The mixture was allowed to drain by gravity. The resin was then washed ten times using high-
259 salt (300 mM NaCl) TBS-A with 8 mM imidazole and 0.05% DDM and subsequently eluted using TBS-A
260 with 200 mM imidazole and 0.05% DDM.

261 **Palmitic acid uptake**

262 The palmitic acid uptake assay was adapted from (12). Briefly, *M. smegmatis* cells were grown to stationary
263 phase in Sauton's medium with palmitate as the carbon source. The cells were pelleted and resuspended
264 in PBS (10 mM Na_2HPO_4, 1.8 mM KH_2PO_4, 2.7 mM KCl, 137 mM NaCl, pH 7.4) supplemented with 0.05%
265 Triton X-100 and 0.1% fatty acid-free bovine serum albumin (BSA) yielding a final OD_{600} of 0.8. After [^{14}C]-

266 palmitic acid (Perkin Elmer) was added, the cells were incubated at 37 ºC with shaking. Cells were
267 harvested at different time points by centrifugation and washed once with ice-cold PBS containing Triton
268 X-100 and BSA. The cells were finally resuspended in the same buffer and aliquoted into plastic
269 scintillation vials for counting using a MicroBeta2 microplate counter (Perkin Elmer).
270

271 **Acknowledgements**

272 We thank Jia Fu Erh and Wei Shen Ho (National University of Singapore) for constructing plasmids and
273 early affinity purification attempts. We are grateful to Beijing Genomics Institute (BGI) Research for
274 providing DNA synthesis and assembly support. We thank Ross Tomaino (Taplin MS facility, Harvard
275 Medical School) for help with protein identification. This work was supported sequentially by the Singapore
276 Ministry of Education Academic Research Fund Tier 2 grants (MOE2019-T2-1-128 and MOE000116) (to
277 S.-S.C.).
278

279 **References**

280 1. World Health Organization, Global Tuberculosis Report 2021, (2021).
281 2. R. M. Houben, P. J. Dodd, The global burden of latent tuberculosis infection: a re-estimation using
282 mathematical modelling. *PLoS Med.* **13**, e1002152 (2016).
283 3. Q. Chai, Y. Zhang, C. H. Liu, *Mycobacterium tuberculosis*: an adaptable pathogen associated with
284 multiple human diseases. *Front. Cell. Infect. Microbiol.* **8**, 158 (2018).
285 4. M. A. Forrellad *et al.*, Virulence factors of the *Mycobacterium tuberculosis* complex. *Virulence* **4**, 3-66
286 (2013).
287 5. L. I. Klepp, J. S. y Sabio, F. Bigi, Mycobacterial MCE proteins as transporters that control lipid
288 homeostasis of the cell wall. *Tuberculosis (Edinb)* **132**, 102162 (2022).
289 6. N. Casali, L. W. Riley, A phylogenomic analysis of the *Actinomycetales mce* operons. *BMC Genomics*
290 **8**, 60 (2007).
291 7. N. Shimono *et al.*, Hypervirulent mutant of *Mycobacterium tuberculosis* resulting from disruption of the
292 *mce1* operon. *Proc. Natl. Acad. Sci. U. S. A.* **100**, 15918-15923 (2003).
293 8. A. Gioffre *et al.*, Mutation in *mce* operons attenuates *Mycobacterium tuberculosis* virulence. *Microbes*

294 *Infect.* **7**, 325-334 (2005).
295 9. A. K. Pandey, C. M. Sassetti, Mycobacterial persistence requires the utilization of host cholesterol.
296 *Proc. Natl. Acad. Sci. U. S. A.* **105**, 4376-4380 (2008).
297 10. R. H. Senaratne *et al.*, *Mycobacterium tuberculosis* strains disrupted in *mce3* and *mce4* operons are
298 attenuated in mice. *J. Med. Microbiol.* **57**, 164-170 (2008).
299 11. M. A. Forrellad *et al.*, Role of the Mce1 transporter in the lipid homeostasis of *Mycobacterium*
300 *tuberculosis*. *Tuberculosis (Edinb)* **94**, 170-177 (2014).
301 12. E. V. Nazarova *et al.*, Rv3723/LucA coordinates fatty acid and cholesterol uptake in *Mycobacterium*
302 *tuberculosis*. *eLife* **6** (2017).
303 13. L. Rank, L. E. Herring, M. Braunstein, Evidence for the mycobacterial mce4 transporter being a
304 multiprotein complex. *J. Bacteriol.* **203**, e00685-00620 (2021).
305 14. N. Casali, A. M. White, L. W. Riley, Regulation of the *Mycobacterium tuberculosis mce1* operon. *J.*
306 *Bacteriol.* **188**, 441-449 (2006).
307 15. M. P. Santangelo *et al.*, Study of the role of Mce3R on the transcription of *mce* genes of *Mycobacterium*
308 *tuberculosis*. *BMC Microbiol.* **8**, 38 (2008).
309 16. J. C. Malinverni, T. J. Silhavy, An ABC transport system that maintains lipid asymmetry in the Gram-
310 negative outer membrane. *Proc. Natl. Acad. Sci. U. S. A.* **106**, 8009-8014 (2009).
311 17. X. Tang *et al.*, Structural insights into outer membrane asymmetry maintenance in Gram-negative
312 bacteria by MlaFEDB. *Nat. Struct. Mol. Biol.* **28**, 81-91 (2021).
313 18. W.-Y. Low, S. Thong, S.-S. Chng, ATP disrupts lipid-binding equilibrium to drive retrograde transport
314 critical for bacterial outer membrane asymmetry. *Proc. Natl. Acad. Sci. U. S. A.* **118** (2021).
315 19. S. Thong *et al.*, Defining key roles for auxiliary proteins in an ABC transporter that maintains bacterial
316 outer membrane lipid asymmetry. *eLife* **5** (2016).
317 20. D. C. Ekiert *et al.*, Architectures of Lipid Transport Systems for the Bacterial Outer Membrane. *Cell*
318 **169**, 273-285 e217 (2017).
319 21. S. M. Joshi *et al.*, Characterization of mycobacterial virulence genes through genetic interaction
320 mapping. *Proc Natl Acad Sci U S A* **103**, 11760-11765 (2006).
321 22. J. Garcia-Fernández, K. Papavinasasundaram, B. Galán, C. M. Sassetti, J. L. García, Unravelling the

322 pleiotropic role of the MceG ATPase in *Mycobacterium smegmatis*. *Environ. Microbiol.* **19**, 2564-2576
323 (2017).
324 23. C. Liu, J. Ma, J. Wang, H. Wang, L. Zhang, Cryo-EM structure of a bacterial lipid transporter YebT. *J.*
325 *Mol. Biol.* **432**, 1008-1019 (2020).
326 24. G. L. Isom *et al.*, LetB structure reveals a tunnel for lipid transport across the bacterial envelope. *Cell*
327 **181**, 653-664 (2020).
328 25. R. Evans *et al.*, Protein complex prediction with AlphaFold-Multimer. BioRxiv [Preprint] (2022).
329 https://www.biorxiv.org/content/10.1101/2021.10.04.463034v2 (accessed 6 June 2022).
330 26. J. Jumper *et al.*, Highly accurate protein structure prediction with AlphaFold. *Nature* **596**, 583-589
331 (2021).
332 27. M. Mirdita *et al.*, ColabFold: making protein folding accessible to all. *Nat. Methods* 10.1038/s41592-
333 022-01488-1 (2022).
334 28. C. Zhou *et al.*, Structural insight into phospholipid transport by the MlaFEBD complex from *P.*
335 *aeruginosa*. *J. Mol. Biol.* **433**, 166986 (2021).
336 29. M. A. Cianfrocco, M. Wong, C. Youn, R. Wagner, A. E. Leschziner, "COSMIC²: A science gateway for
337 cryo-electron microscopy structure determination" in *Proceedings of the Practice and Experience in*
338 *Advanced Research Computing 2017 on Sustainability, Success and Impact* (Association for
339 Computing Machinery, New York, NY, 2017), pp. 1-5.
340 30. R. R. Crawford, P. K. Potukuchi, E. G. Schuetz, J. D. Schuetz, Beyond competitive inhibition: regulation
341 of ABC transporters by kinases and protein-protein interactions as potential mechanisms of drug-drug
342 interactions. *Drug Metab. Dispos.* **46**, 567-580 (2018).
343 31. N. S. Kadaba, J. T. Kaiser, E. Johnson, A. Lee, D. C. Rees, The high-affinity *E. coli* methionine ABC
344 transporter: structure and allosteric regulation. *Science* **321**, 250-253 (2008).
345 32. S. Gerber, M. Comellas-Bigler, B. A. Goetz, K. P. Locher, Structural basis of trans-inhibition in a
346 molybdate/tungstate ABC transporter. *Science* **321**, 246-250.
347 33. S. Chen, M. L. Oldham, A. L. Davidson, J. Chen, Carbon catabolite repression of the maltose
348 transporter revealed by X-ray crystallography. *Nature* **499**, 364-368 (2013).
349 34. S. B. Ko *et al.*, Gating of CFTR by the STAS domain of SLC26 transporters. *Nat. Cell. Biol.* **6**, 343-350

350 (2004).

351 35. V. D. Nikitushkin *et al.*, The main pigment of the dormant *Mycobacterium smegmatis* is porphyrin.
352 *FEMS Microbiol. Lett.* **363** (2016).

353 36. W. Lee, B. C. VanderVen, R. J. Fahey, D. G. Russell, Intracellular Mycobacterium tuberculosis exploits
354 host-derived fatty acids to limit metabolic stress. *J. Biol. Chem.* **288**, 6788-6800 (2013).

355 37. A. Martin, J. Daniel, The ABC transporter Rv1272c of *Mycobacterium tuberculosis* enhances the import
356 of long-chain fatty acids in *Escherichia coli*. *Biochem. Biophys. Res. Commun.* **496**, 667-672 (2018).

357

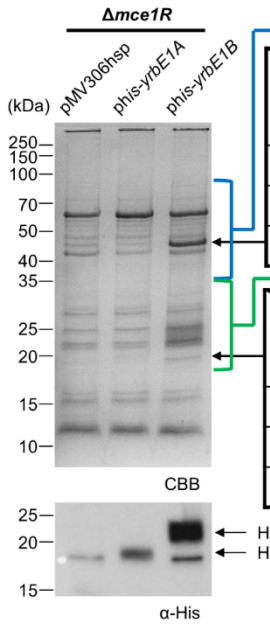

Protein (kDa) \ Lane	# peptides detected (MS) from the gel band	
	pMV306	*phis-yrbE1B*
MceG (39.0)	**1**	**132**
GroL2 (56.5)	28	46
AtpFH (47.4)	14	32

Protein (kDa) \ Lane	# peptides detected (MS) from the gel band	
	pMV306	*phis-yrbE1B*
Msmeg_0959 (19.1)	**1**	**35**
Msmeg_5838 (19.2)	5	5
GroL2 (56.5)	1	4

Protein (kDa) \ Lane	# peptides detected (MS) from the gel section	
	pMV306	*phis-yrbE1B*
MceG (39.0)	1	225
Mce1B (37.4)	0	27
Mce1C (54.7)	0	25
Mce1E (42.5)	0	21
Msmeg_6112 (39.0)	0	20
Msmeg_6540 (45.1)	0	16
Mce1D (58.0)	0	15
YrbE1B (30.8)	0	14
Mce1F (54.3)	0	14
Msmeg_4715 (41.3)	0	11
Mce1A (43.9)	0	11

Protein (kDa) \ Lane	# peptides detected (MS) from the gel section	
	pMV306	*phis-yrbE1B*
YrbE1B (30.8)	0	149
Msmeg_0959 (19.1)	0	115
YrbE4A (26.6)	0	13
YrbE1A (27.7)	0	12

358

359 **Figure 1. Affinity purification with His$_6$-YrbE1B defines the composition of Mce1 complexes.** SDS-
360 PAGE and α-His immunoblot analyses of proteins affinity-purified from *M. smegmatis* Δ*mce1R* cells
361 expressing His-tagged YrbE1A (p*his-yrbE1A*) or YrbE1B (p*his-yrbE1B)*. pMV306hsp was used as the
362 empty vector control. For protein identification from gel bands, the top three proteins detected in the p*his-*
363 *yrbE1B* lane are listed. For protein identification from gel sections (blue: 35–90 kDa, green: 18–35 kDa),
364 proteins with more than ten total peptides detected and significantly enriched in the p*his-yrbE1B* lane are
365 listed. CBB, Coomassie brilliant blue.

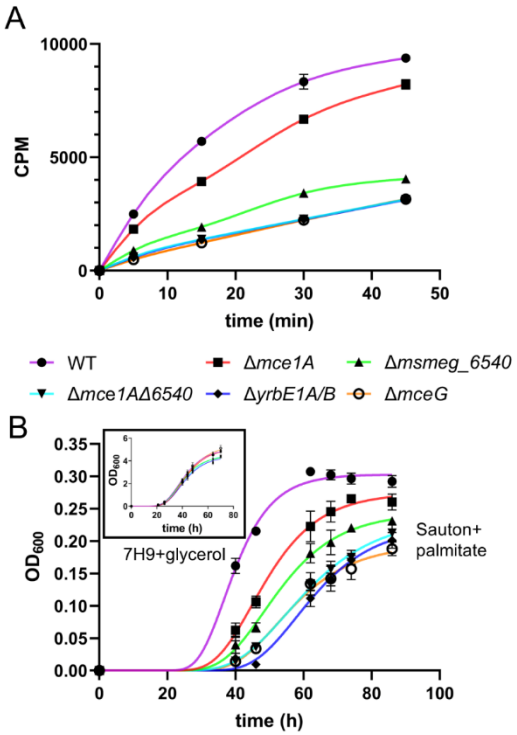

366

367 **Figure 2. Both Msmeg_6540 and Mce1A are important for fatty acid uptake. (A)** [^{14}C]-palmitic acid
368 uptake kinetics of indicated *M. smegmatis* strains. Each data point (mean ± standard deviation) represents
369 results from three technical replicates. The uptake profiles are representative of at least three independent
370 experiments. **(B)** Growth curves of the same strains in **(A)** in Sauton's medium containing palmitate as the
371 sole carbon source or (inset) 7H9 medium containing glycerol. Each data point (mean ± standard deviation)
372 represents results from three biological replicates.

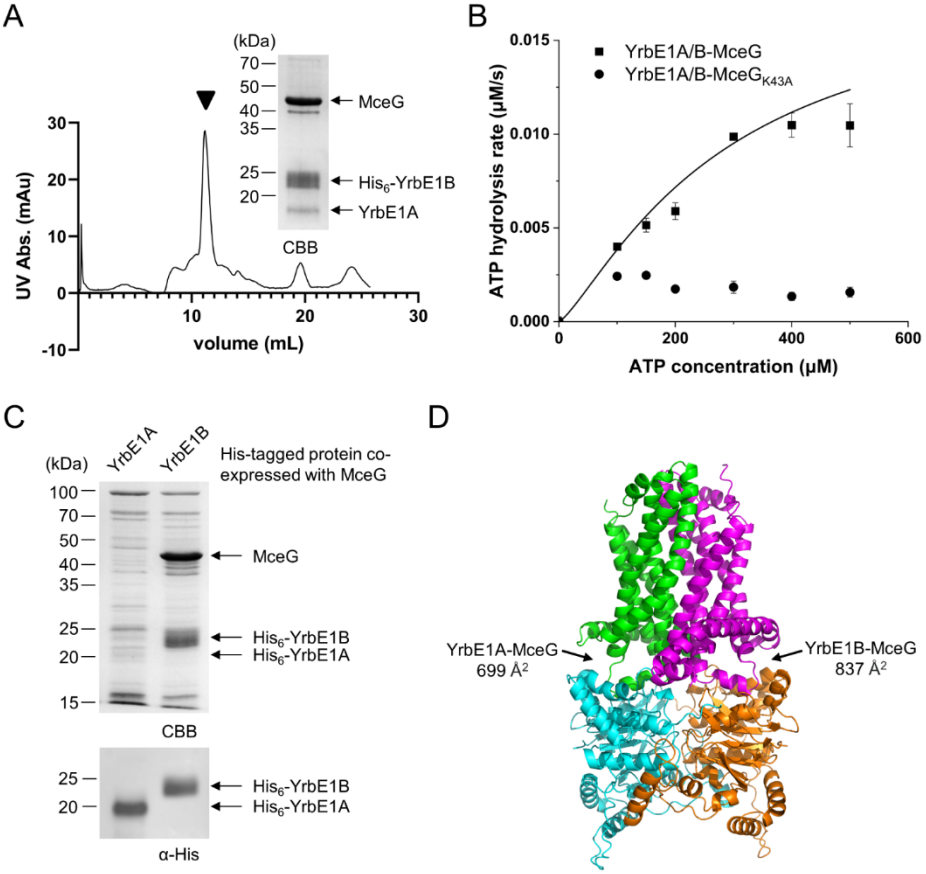

Figure 3. YrbE1A/B-MceG form a stable asymmetric complex with ATPase activity. (A) Size exclusion chromatographic profile of the purified complex comprising YrbE1A, His_6-YrbE1B and MceG. SDS-PAGE analysis of the peak corresponding to the complex (black arrow head) is shown. **(B)** Enzyme-coupled ATPase assay of 0.1 μM YrbE1A/B-MceG and YrbE1A/B-$MceG_{K43A}$ in detergent micelles at 37 ºC. Average ATP hydrolysis rates from three technical triplicates were plotted against ATP concentrations, and fitted to an expanded Michaelis-Menten equation that includes a term for Hill coefficient (n). YrbE1A/B-MceG: K_m = 284 ± 311μM, k_{cat} = 0.184 ± 0.125 μM ATP s^{-1}/μM complex, n = 1.28 ± 0.57. The data for the mutant failed to fit to the equation with significant confidence. Each data point is shown as mean ± standard deviation. **(C)** SDS-PAGE and α-His immunoblot analyses of proteins affinity-purified from *E. coli* cells over-expressing His_6-YrbE1A or His_6-YrbE1B together with MceG. CBB, Coomassie brilliant blue. **(D)** An AlphaFold2 structural model of the YrbE1A/B-MceG complex (*green*: YrbE1A, *magenta*: YrbE1B, *cyan* and *orange*: MceG), with respective calculated interface areas indicated.

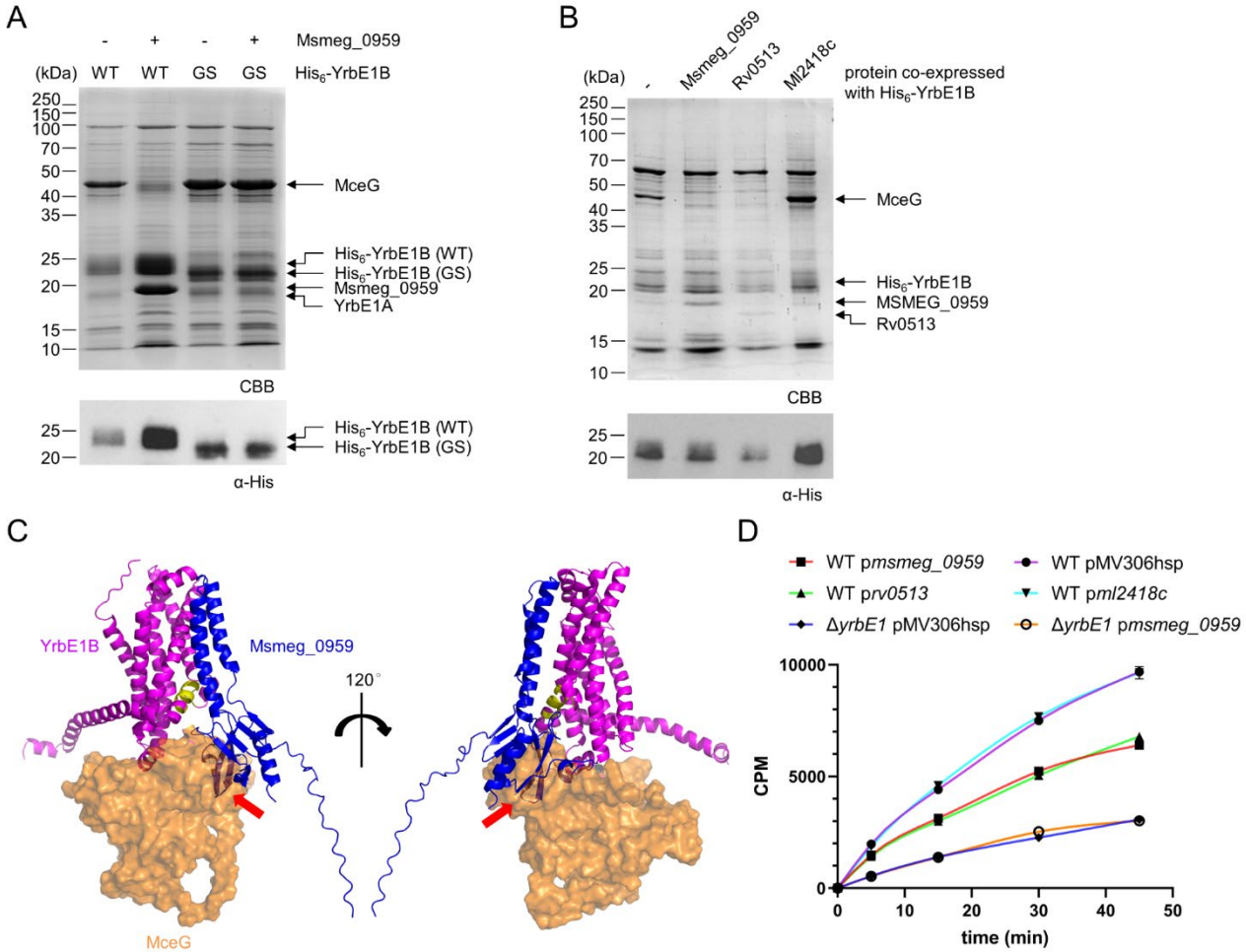

Figure 4. Msmeg_0959 negatively regulates the Mce1 transporter. (A) SDS-PAGE and α-His immunoblot analyses of proteins affinity-purified from *E. coli* cells over-expressing YrbE1A, MceG, and either wild-type His_6-YrbE1B (WT) or the helix-to-loop mutant His_6-YrbE1B (GS), in the presence (+) or absence (-) of Msmeg_0959. **(B)** SDS-PAGE and α-His immunoblot analyses of proteins affinity-purified from *M. smegmatis* cells over-expressing Mce1N from different species (Rv0513 from *M. tuberculosis* and Ml2418c from *M. leprae*) and His_6-YrbE1B as the bait protein. **(C)** An overlay of AlphaFold2 models of YrbE1B (*magenta*)-MceG (*orange* surface) and YrbE1B-Msmeg_0959 (*blue*). The helix-to-loop mutation located on the putative short helix at the YrbE1B-Msmeg_0959 interface is highlighted in *yellow*. The steric clash between MceG and Msmeg_0959 is indicated by *red* arrows. **(D)** [^{14}C]-palmitic acid uptake kinetics of indicated *M. smegmatis* strains overexpressing Mce1N from different mycobacterial species. Each data point (mean ± SD) represents results from three technical replicates. The uptake profiles are representative of three independent experiments.

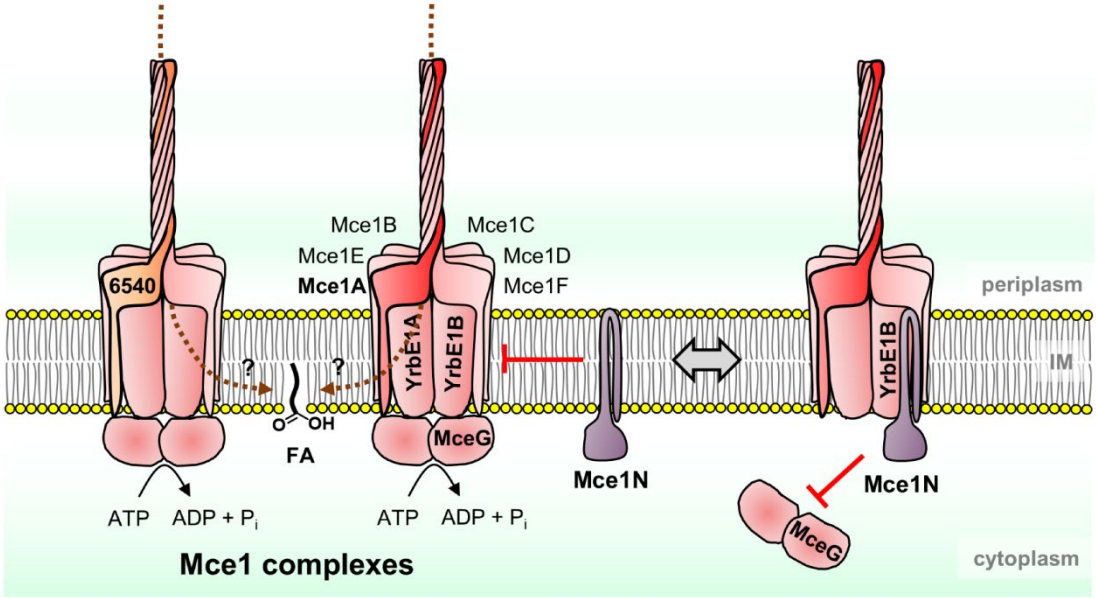

Figure 5. A proposed model of Mce1 complexes and their regulation by Mce1N. Mce1 complexes are ABC transporters for fatty acids, with YrbE1A/B as TMDs, MceG as NBDs, and heterohexameric MCE-domain proteins as SBPs. There are two variants of Mce1 complexes in *M. smegmatis*, each containing Msmeg_6540 or Mce1A in addition to Mce1B–F. The relative order of protomers within heterohexameric SBP complexes is indicated based on the AlphaFold2 models (*SI Appendix*, Fig. S5*B*). Mce1N is a negative regulator of the Mce1 system; it specifically binds to YrbE1B and prevents its interaction with MceG.